



Original scientific paper

## Electrochemical investigation of the corrosion behavior of heat treated Al-6Si-0.5Mg-xCu (x=0, 0.5 and 1) alloys

Abul Hossain✉, Mohammed Abdul Gafur\*, Fahmida Gulshan and Abu Syed Wais Kurny

Department of Materials and Metallurgical Engineering, Bangladesh University of Engineering and Technology, Dhaka, Bangladesh

\*Pilot Plant and Process Development Centre (PP & PDC), BCSIR Laboratories, Dhaka, Bangladesh

✉Corresponding Author: [ah\\_buetmmesgfl@live.com](mailto:ah_buetmmesgfl@live.com); Tel.: +88-01711243601

Received: June 23, 2014; Revised: December 31, 2014; Published: March 15, 2015

### Abstract

The corrosion behavior of heat treated Al-6Si-0.5Mg-xCu (x=0, 0.5 and 1 wt %) alloys in 0.1 M NaCl solution was investigated using potentiodynamic polarization and electrochemical impedance spectroscopy (EIS) techniques. The potentiodynamic polarization curves reveal that 0.5 wt % Cu and 1 wt % Cu content alloys are less prone to corrosion than the Cu free alloy. The EIS test results also showed that corrosion resistance or charge transfer resistance ( $R_{ct}$ ) increases with increasing Cu content into Al-6Si-0.5Mg alloy. Maximum charge transfer resistance ( $R_{ct}$ ) was obtained with the addition of 1 wt % Cu and minimum  $R_{ct}$  value was for Cu free Al-6Si-0.5Mg alloy. Due to addition of Cu and thermal modification, the magnitude of open circuit potential (OCP), corrosion potential ( $E_{corr}$ ) and pitting corrosion potential ( $E_{pit}$ ) of Al-6Si-0.5Mg alloy in NaCl solution were shifted to the more noble direction.

### Keywords

Al alloy; Nyquist plot; Corrosion rate; Tafel plot; EIS

### Introduction

Aluminium and its alloys are considered to be highly corrosion resistant under the majority of service conditions [1]. The various grades of pure aluminum are the most resistant, followed closely by the Al-Mg and Al-Mn alloys. Next in order are Al-Mg-Si and Al-Si alloys. The alloys containing copper are the least resistant to corrosion [2]; but this can be improved by coating each side of the copper containing alloy with a thin layer of high purity aluminium, thus gaining a three

ply metal (Alclad). This cladding acts as a mechanical shield and offers sacrificial protection [3]. When aluminum surfaces are exposed to atmosphere, a thin invisible oxide ( $\text{Al}_2\text{O}_3$ ) skin forms, which protects the metal from further corrosion in many environments [1]. This film protects the metal from further oxidation unless this coating is destroyed, and the material remains fully protected against corrosion [3]. The composition of an alloy and its thermal treatment are important do determine the susceptibility of the alloy to corrosion [4,5].

Over the years a number of studies have been carried out to assess the effect of Cu content and the distribution of second phase intermetallic particles on the corrosion behavior of Al alloys. The distribution of Cu in the microstructure affects the susceptibility to localized corrosion. Intergranular corrosion (IGC) is generally believed to be associated with Cu containing grain boundary precipitates and the precipitates free zones (PFZ) along grain boundaries [6-8]. In heat treatable Al-Si-Mg(-Cu) series alloys the susceptibility to localized corrosion (pitting and / or intergranular (IGC)) and the extent of attack are mainly controlled by the type, amount and distribution of the precipitates which form in the alloy during any thermal or thermomechanical treatment performed during manufacturing processes [6-10].

Depending on the composition of the alloy and parameters of the heat treatment process, these precipitates form in the bulk of the grain, or in the bulk as well as grain boundaries. As indicated by several authors, the precipitates formed by heat treatment in Al-Si-Mg alloys containing Cu are the  $\theta$  ( $\text{Al}_2\text{Cu}$ ) Q-phase ( $\text{Al}_4\text{Mg}_8\text{Si}_7\text{Cu}_2$ ),  $\beta$ -phase ( $\text{Mg}_2\text{Si}$ ) and free Si if Si content in the alloy exceeds the  $\text{Mg}_2\text{Si}$  stoichiometry [2-12].

The present study is an attempt to investigate the corrosion behavior of Al-6Si-0.5Mg alloys containing 0.5 and 1 wt % Cu in 0.1M NaCl solution and to examine corroded surfaces by optical and scanning electron microscopy.

## Experimental

**Materials preparation:** The Al-6Si-0.5Mg-xCu(x= 0, 0.5 and 1) alloys were prepared by melting Al-7Si-0.3Mg (A356) alloys and adding Al and Cu into the melt. The melting operation was carried out in a gas fired clay graphite crucible furnace and the alloys were cast in a permanent steel mould. After solidification the alloys were homogenised (500 °C for 24 hr), solution treated (540 °C for 2 hr) and finally artificially aged (225 °C for 1 hr). After heat treatment rectangular samples (30x10x5 mm) were prepared for metallographic observation and subsequent electrochemical test. Deionized water and analytical reagent grade sodium chloride (NaCl) were used for the preparation of 0.1 M solution. All measurements were carried out at room temperature.

**Potentiodynamic polarization measurements:** A computer-controlled Gamry Framework TM Series G 300™ and Series G 750™ Potentiostat/Galvanostat/ZRA were used for the electrochemical measurements. The potentiodynamic polarization studies were configured in cells, using three-electrode assembly: a saturated calomel reference electrode, a platinum counter electrode and the sample in the form of coupons of exposed area of 0.50 cm<sup>2</sup> or 10 x 5 mm as working electrode. Only one 10x5 mm surface was exposed to the test solution, the other surfaces being covered with Teflon tape. The system was allowed to establish a steady-state open circuit potential (OCP). The potential range selected was -1 to +1V and measurements were made at a scan rate of 0.50 mV/s. The corrosion current ( $I_{\text{corr}}$ ), corrosion potential ( $E_{\text{corr}}$ ), pitting corrosion potential ( $E_{\text{pit}}$ ) and corrosion rate (mm/year) were calculated from Tafel curve. The tests were carried out at room temperature in 0.1 M NaCl solutions at a fixed and neutral pH value. The corroded samples were cleaned in distilled water and examined under optical light and scanning electron microscope.

**Electrochemical impedance measurements:** As in potentiodynamic polarization test, three electrode cell arrangements were also used in electrochemical impedance measurements. Rectangular samples (10 x 5 mm) were connected with copper wire and adopted as working electrode. EIS tests were performed in 0.1M NaCl solution at room temperature over a frequency range of 100 kHz to 0.2 Hz using a 5 mV amplitude sinusoidal voltage. The 10 x 5 mm sample surface was immersed in 0.1M NaCl solution (corrosion medium). All the measurements were performed at the open circuit potential (OCP). The test cells were maintained at room temperature and the NaCl solution was refreshed regularly during the whole test period. The impedance spectra were collected, fitting the experimental results to an equivalent circuit (EC) using the Echem Analyst TM data analysis software and evaluating the solution resistance ( $R_s$ ), polarization resistance or charge transfer resistance ( $R_{ct}$ ) and double layer capacitance ( $C_p$ ) of the thermal treated alloys.

## Results and discussion

### Impedance measurements

Table 1 shows the electrochemical impedance spectroscopy (EIS) test results.

**Table 1.** Impedance test results

Alloy Code	Alloy Compositions	$R_s / \Omega$	$R_{ct} / k\Omega$	$C_p / \mu F$	OCP, V vs. SCE
Alloy-1	Al-6Si-0.5Mg	40.37	15.57	1.259	-0.8454
Alloy-2	Al-6Si-0.5Mg-0.5Cu	43.93	25.75	1.793	-0.7037
Alloy-3	Al-6Si-0.5Mg-1Cu	44.08	27.13	3.219	-0.6534

### OCP versus time behavior

The open circuit potential (OCP) with exposure time of aged Al-6Si-0.5Mg-xCu alloys in 0.1 M NaCl solution is shown in Table1. Large fluctuations in open circuit potential for the alloys were seen during the time of 100 s exposure. After a period of exposure the OCP fluctuation decreased and reached steady state. The steady state OCP of Cu free alloy (Alloy-1) is -0.8454 V and it is the most negative OCP value among the alloys under investigation. The occurrence of a positive shift in OCP in the Al-6Si-0.5Mg alloys containing 0.5 and 1.0 % Cu indicates the existence of anodically controlled reaction. The OCP values mainly depend on the chemical compositions and thermal history of the alloys.

The data obtained were modeled and the equivalent circuit that best fitted to the experimental data is shown in Figure 1.  $R_s$  represent the ohmic solution resistance of the electrolyte.  $R_{ct}$  and  $C_p$  are the charge transfer resistance and electrical double layer capacitance respectively, which correspond to the Faradaic process at the alloy/media interface.

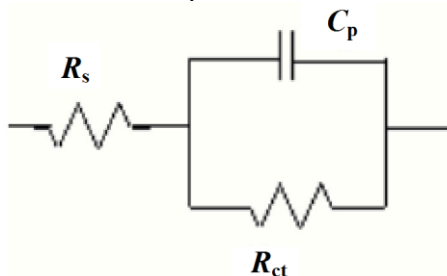


**Figure 1.** Electrical equivalent circuit used for fitting of the impedance data of Al-6Si 0.5Mg-xCu alloys in 0.1M NaCl solution.

Figure 2 shows the Nyquist diagrams (suggested equivalent circuit model shown in Figure 1) of the Al-6Si-0.5Mg-xCu alloys in 0.1M NaCl in de-mineralized (DM) water. In Nyquist diagrams, the imaginary component of the impedance ( $Z''$ ) against real part ( $Z'$ ) is obtained in the form of capacitive-resistive semicircle for each sample.

Figure 3 shows the experimental EIS results in Bode magnitude diagram for Al-6Si-0.5Mg-xCu alloys. Bode plots show the total impedance behaviour against applied frequency. At high frequencies, only the very mobile ions in solution are excited so that the solution resistance ( $R_s$ ) can be assessed. At lower intermediate frequencies, capacitive charging of the solid-liquid interface occurs. The capacitive value  $C_p$  can provide very important information about oxide properties when passivation or thicker oxides are formed on the surface. At low frequency, the capacitive charging disappears because the charge transfer of electrochemical reaction can occur and this measured value of the resistance corresponds directly to the corrosion rate. For this reason, this low frequency impedance value is referred to as polarization or charge transfer resistance ( $R_{ct}$ ).

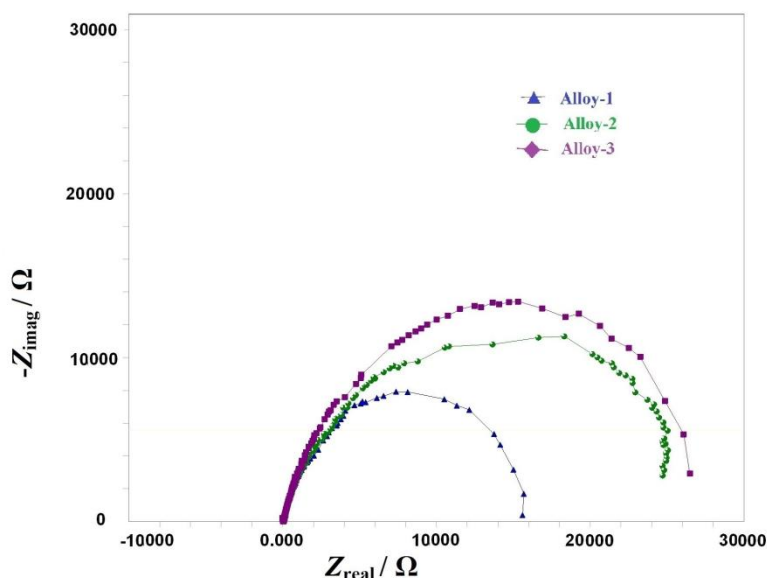


Figure 2. Nyquist plots for the peak-aged Alloys 1, 2 and 3 in 0.1M NaCl solution.

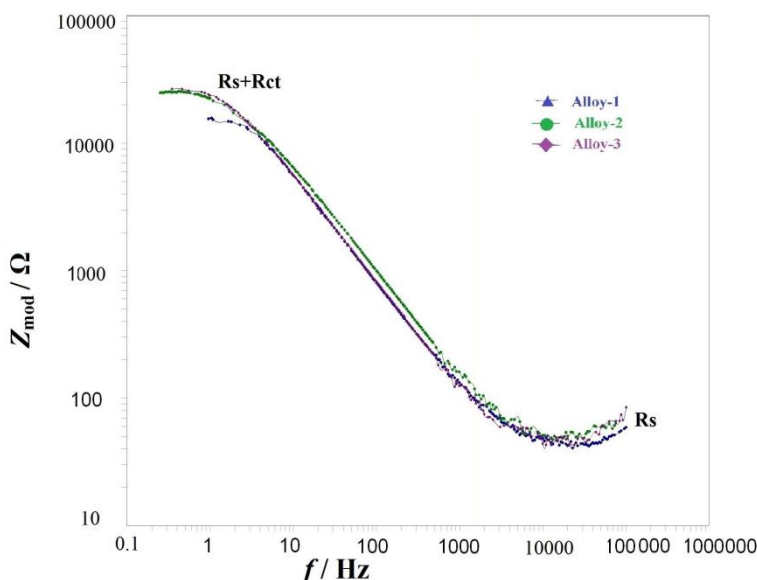


Figure 3. Bode plots for the peak-aged Alloys 1, 2 and 3 in 0.1M NaCl solution.

The solution resistance ( $R_s$ ) of the alloys varies from 40-44  $\Omega$  (Table 1) and these values are very similar to each other. So there are insignificant changes of  $R_s$  values for the alloys during EIS testing. The  $R_s$  values are negligible with respect to  $R_{ct}$  and the electrolyte behaves as a good ionic conductor. Impedance measurements showed that in 0.1M NaCl solution, increasing Cu in the Al-6Si-0.5Mg alloys increases the charge transfer resistance ( $R_{ct}$ ). For the Cu free Al-6Si-0.5Mg alloy (Alloy-1), the charge transfer resistance ( $R_{ct}$ ) value in 0.1M NaCl solution is 15.57 k $\Omega$ , and this is increased to 25.75 and 27.13 k $\Omega$  with the addition of 0.5 and 1 wt % Cu to the Al-6Si-0.5Mg alloy respectively. The increase in the charge transfer resistance indicates an increase in the corrosion resistance of the alloys with Cu addition. The double layer capacitance ( $C_p$ ) of the Cu free Al-6Si-0.5 Mg alloy (Alloy-1) is 1.259  $\mu\text{F}$ , which is the lowest value among the alloys investigated. The double layer capacitance of Al-6Si-0.5Mg alloy increased with an increase in Cu content and the maximum was found for Alloy-3.

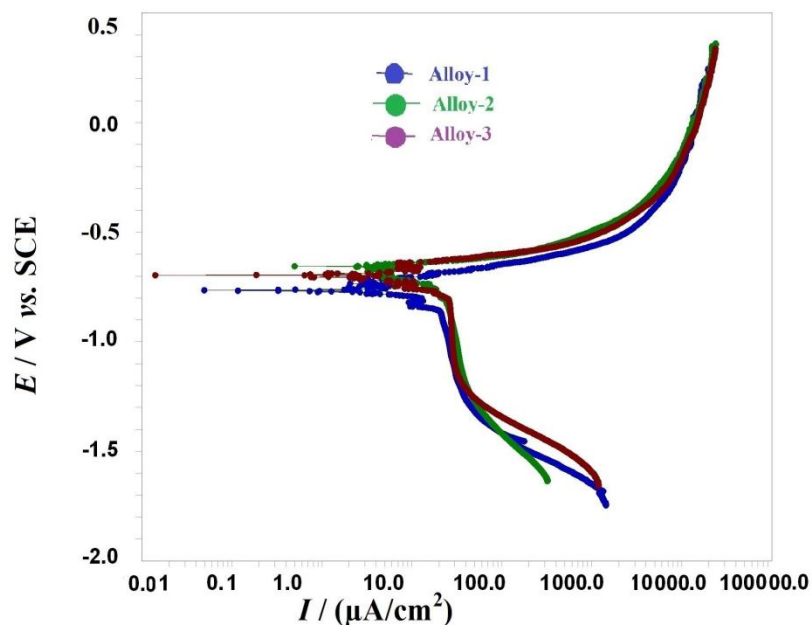
#### Potentiodynamic polarization measurements

Table 2 shows the potentiodynamic polarization test results obtained from the electrochemical tests.

**Table 2.** Potentiodynamic polarization test results

Alloy code	$I_{\text{corr}} / \mu\text{A}$	$E_{\text{corr}} / \text{mV}$	$E_{\text{pit}} / \text{mV}$	Corrosion rate, mm/year
Alloy-1	6.300	-764	-480	5.287
Alloy-2	5.640	-657	-408	4.732
Alloy-3	2.950	-697	-370	2.474

Potentiodynamic polarization curves of Al-6Si-0.5Mg-xCu alloys in 0.1M NaCl solution are shown in Figure 4. Anodic current density of Al-6Si-0.5Mg-xCu alloys decreased with Cu addition. This is caused by the slowing of the anodic reaction of Al-6Si-0.5Mg-xCu alloy.



**Figure 4.** Potentiodynamic polarization curves of packaged Alloys 1, 2 and 3 in 0.1M NaCl solution.

The addition of Cu caused the formation of micro-galvanic cells in  $\alpha$ -aluminum matrix. The different intermetallic compounds (like  $\text{Mg}_2\text{Si}$ ,  $\text{Al}_2\text{Cu}$  etc.) can lead to the formation of micro-

galvanic cells because of the difference of corrosion potential between intermetallics and  $\alpha$ -aluminum matrix. Park [13] has also reported that the addition of Cu increased the corrosion potential of a number of Al-Cu-Si alloys. For the Cu free Al-6Si-0.5Mg alloy (Alloy-1) corrosion potential is -764 mV, which is the highest negative potential among the alloys investigated. With increasing Cu, the corrosion potential of the alloys shifted towards more positive values. Pitting potential (Epit) of all Cu content alloys also shifted towards more positive values (from -480 mV to -370 mV). Potentiodynamic tests showed that in 0.1M NaCl solution, increasing Cu in the Al-6Si-0.5Mg alloy decreases the corrosion current ( $I_{corr}$ ). For the Cu free Al-6Si-0.5Mg alloy (Alloy-1), the corrosion current ( $I_{corr}$ ) value in 0.1M NaCl solution is 6.3  $\mu$ A, and this decreased to 5.640 and 2.950  $\mu$ A with the addition of 0.5 and 1 wt % Cu to the Al-6Si-0.5Mg alloy respectively and the corresponding corrosion rate decreases for these alloys (Alloy-2 = 4.732 mpy and Alloy-3 = 2.474 mm/year).

### Microstructural Investigation

The microstructure of some selected as-corroded samples was observed under OLM and SEM. There was evidence of corrosion products of intermetallic compounds in all the samples examined. Besides, several pits were visible in all the samples examined. It is probable that the pits are formed by the intermetallics dropping out from the surface due to the dissolution of the surrounding matrix. However, it is also possible that the pits are caused by selective dissolution of the intermetallic/or particles of the second phase precipitates.

Osorio *et al.* [14] have demonstrated that in Al-Cu-Si alloys a more finely and homogeneously distributed  $Al_2Cu$  and needle-like Si particles in the ternary eutectic mixture, tend to improve the corrosion resistance mainly due to the galvanic protection of both  $Al_2Cu$  and Si phases [14]. Although it has also been reported [14,15] that fine Si particles tends to decrease the corrosion resistance of binary Al-Si alloys when associated with the  $Al_2Cu$  intermetallic phase, a better galvanic protection is provided for finer Al-Cu-Si alloy microstructures. It was also reported [16] that the ternary eutectic mixture consisting of Al +  $Al_2Cu$  + Si phases is nobler than the Al-matrix and Al-phase in the eutectic mixture [16].

Consequently, the forms of corrosion in the studied Al-6Si-0.5Mg-xCu alloys are slightly uniform and predominantly pitting corrosion as obtained by the OLM and SEM. Samples were characterized by OLM and SEM following potentiodynamic polarization tests. The peakaged Cu free alloy (Alloy-1) exhibited pits on their surface (Figure 5), which apparently had nucleated randomly.

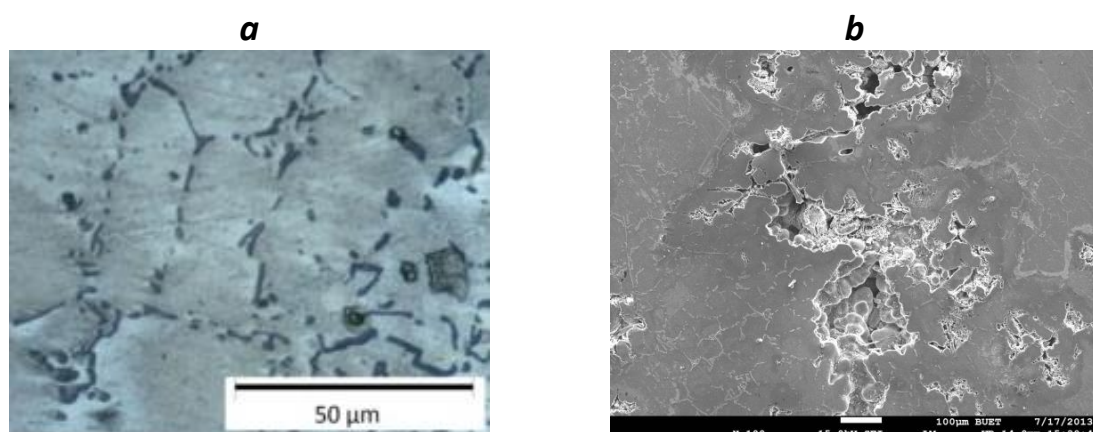


**Figure 5. (a) OLM and (b) SEM images show the damage surface morphology of as-corroded T6 aged Alloy-1 in 0.1M NaCl solution.**

Conversely, the exposed surface of the alloys exhibited a corrosion product with a rippled appearance covering the surface after polarization. All the optical micrographs (Figures 5-6) also showed that there was no corrosion in the fragmented and modified Al-Si eutectics.

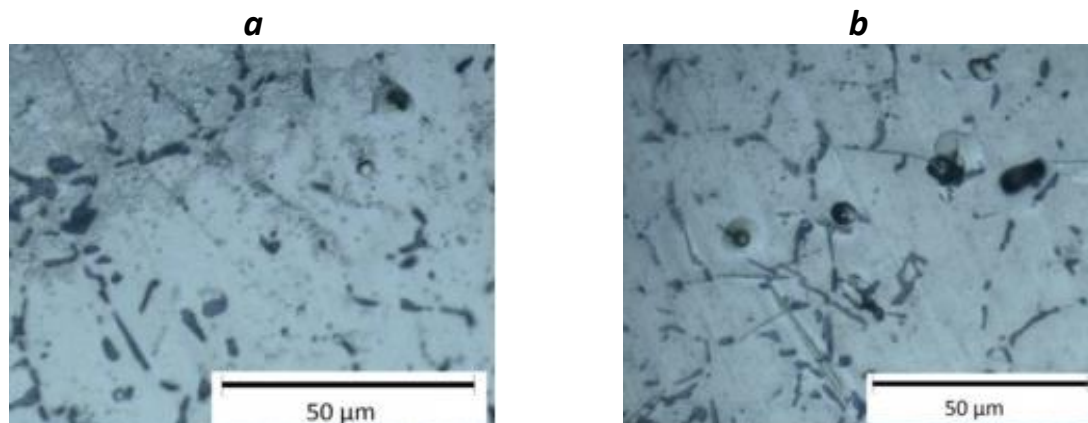


**Figure 6.** OLM images of the damage surfaces morphology of as-corroded T6 aged **(a)** Alloy-2 and **(b)** Alloy-3 in 0.1M NaCl solution.

## Conclusions

The following conclusions may be drawn from the above investigation:

1. The EIS tests have shown that the additions of Cu into Al-Si-Mg alloy tend to increase the excellent corrosion resistance of Al-Si-Mg alloy in NaCl media. The corrosion resistance,  $R_{ct}$  value of the alloys shows a maximum at 1 wt % Cu.
2. The linear polarization and Tafel extrapolation plot show that the corrosion current ( $I_{corr}$ ) and corrosion rate (mm/year) decrease with increasing of Cu content into Al-6Si-0.5Mg alloy. The open circuit potential (OCP), corrosion potential ( $E_{corr}$ ) and pitting corrosion potential ( $E_{pit}$ ) in the NaCl solution were shifted in the more noble direction due to Cu additions into Al-6Si-0.5Mg alloy.
3. Consequently, the forms of corrosion in the studied Al-6Si-0.5Mg-xCu alloys are pitting corrosion as obtained from the microstructures study with pits observations.

## References

- [1] M. G. Fontana, N.D. Greene, *Corrosion Engineering*, McGraw-Hill book Company, New York, 1987, 8-29.
- [2] S. Zor, M. Zeren, H. Ozkazance, E. Karakulak, *Anti-Corrosion Methods and Materials* **57** (2010) 185-191.
- [3] G. M. Scamans, J. A. Hunter, N. J. H. Holroyd, , *Proc. of 8<sup>th</sup> Inter. Light metals Congress*, Leoban Wien, 1989, 699-705,
- [4] M. Czechowski, *Adv. Mater Sci.* **7** (2007) 13-20.
- [5] M. Abdulwahab, I.A. Madugu, S.A. Yaro, A.P.I. Popoola, *Journal of Minerals & Materials Characterization & Engineering* **10** (2011) 535-551.
- [6] G. Svenningsen, M.H. Larsen, *Corros. Sci.* **48** (2006) 3969–3987.
- [7] G. Svenningsen, J.E. Lein, A. Bjorgum, J.H. Nordlien, K. Nisancioglu, *Corros. Sci.* **48** (2006) 226-242.
- [8] M. H. Larsen, J. C. Walmsley, *Mater. Sci. Forum* **519-521** (2006) 667-671.
- [9] G. Svenningsen, M.H. Larsen, J.H. Nordlien, K. Nisancioglu, *Corros. Sci.* **48** (2006) 258–272.
- [10] G. Svenningsen, M.H. Larsen, *Corros. Sci.* **48** (2006) 1528–1543.

- [11] H. Zhan, J. M. C. Mo, F. Hannour, L. Zhuang, H. Terryn, J. H. W. de Wit, *Materials and Corrosion* **59** (2008) 670–675.
- [12] M. H. Larsen, J. C. Walmsley, O. Lunder and K. Nisancioglu, *J. Electrochem. Soc.* **157** (2010) 61-68.
- [13] M. Park, *J. Mater. Sci.* **40** (2005) 3945.
- [14] W. R. Osório, D. J. Moutinho, L. C. Peixoto, I. L. Ferreira, A. Garcia. *Electrochimica Acta* **56** (2011) 8412–8421.
- [15] W. R. Osório, N. Cheung, J. E. Spinelli, A. Garcia. *J. Solid State Electrochem* **11(10)** (2007) 1421-1427.
- [16] W. R. Osório, L. C. Peixoto, D. J. Moutinho, L. G. Gomes, I. L. Ferreira, A. Garcia. *Materials and Design* **32** (2011) 3832–3837.

© 2015 by the authors; licensee IAPC, Zagreb, Croatia. This article is an open-access article distributed under the terms and conditions of the Creative Commons Attribution license

<http://creativecommons.org/licenses/by/4.0/>

